

## Structure–Activity Relationships of Cyclic Peptide-Based Chemokine Receptor CXCR4 Antagonists: Disclosing the Importance of Side-Chain and Backbone Functionalities

Satoshi Ueda,<sup>†</sup> Shinya Oishi,<sup>†</sup> Zi-xuan Wang,<sup>‡</sup> Takano Araki,<sup>†</sup> Hirokazu Tamamura,<sup>†,‡</sup> Jérôme Cluzeau,<sup>†</sup> Hiroaki Ohno,<sup>†</sup> Shuichi Kusano,<sup>||</sup> Hideki Nakashima,<sup>||</sup> John O. Trent,<sup>§</sup> Stephen C. Peiper,<sup>‡</sup> and Nobutaka Fujii<sup>†,\*</sup>

Graduate School of Pharmaceutical Sciences, Kyoto University, Sakyo-ku, Kyoto 606-8501, Japan, Department of Pathology, Medical College of Georgia, Georgia 30912, Institute of Biomaterials and Bioengineering, Tokyo Medical and Dental University, Chiyoda-ku Tokyo 101-0062, Japan, St. Marianna University, School of Medicine, Miyamae-ku, Kawasaki 216-8511, Japan, and James Graham Brown Cancer Center, University of Louisville, Kentucky 40202

Received June 19, 2006

Previously, we have identified a highly potent CXCR4 antagonist **2** [cyclo(-D-Tyr<sup>1</sup>-Arg<sup>2</sup>-Arg<sup>3</sup>-Nal<sup>4</sup>-Gly<sup>5</sup>-)] and its Arg<sup>2</sup> epimer **3** [cyclo(-D-Tyr<sup>1</sup>-D-Arg<sup>2</sup>-Arg<sup>3</sup>-Nal<sup>4</sup>-Gly<sup>5</sup>-)] by the screening of cyclic pentapeptide libraries that were designed based on the structure–activity relationship studies on 14-residue peptidic CXCR4 antagonist **1**. In the present study, a new series of analogues of **2** and **3** were synthesized to evaluate the influences of peptide side-chain and backbone modification on bioactivities. Based on the Ala-scanning study, in which each residue in **2** and **3** was replaced with Ala having the identical chirality, substitution of Arg<sup>3</sup> and Nal<sup>4</sup> [Nal = L-3-(2-naphthyl)alanine] with Ala (compounds **6**, **7**, **10**, **11**) led to significant loss of the potency, indicating these amino acids are more important contributors to the bioactivity. For the cyclic peptide backbone, several modifications including D/L-Ala or cyclic amino acids substitution at the Gly<sup>5</sup> position and sequential *N*-methylation on amide nitrogens were conducted. Among the analogues, compounds **13** [cyclo(-D-Tyr<sup>1</sup>-Arg<sup>2</sup>-Arg<sup>3</sup>-Nal<sup>4</sup>-D-Ala<sup>5</sup>-)] and **32** [cyclo(-D-Tyr<sup>1</sup>-D-MeArg<sup>2</sup>-Arg<sup>3</sup>-Nal<sup>4</sup>-Gly<sup>5</sup>-)] were close in potency to the most potent lead **2**. NMR and conformational analysis indicated that both of these analogues favor the same backbone conformation as **2**, whereas similar analysis of less potent analogues indicates that an altered backbone conformation is favored. The conformational analysis showed that steric repulsion by a 1,3-allylic strain-like effect across the planar peptide bond might contribute to the conformational preferences of cyclic pentapeptides.

### Introduction

Chemokines comprise a protein family of chemotactic factors that bind G protein-coupled receptors.<sup>1,2</sup> Engagement of chemokine receptors by their ligands triggers changes of the receptor conformation that lead to the initiation of a signaling cascade involving G protein binding, protein kinase activation, Ca<sup>2+</sup> mobilization from intracellular stores, and cytoskeletal rearrangement, eventually leading to directed cell migration toward the gradients of the respective ligand.<sup>3,4</sup> A chemokine receptor CXCR4 and its endogenous ligand CXCL12 (stromal cell derived factor-1, SDF-1) are partners in multiple important functions in normal physiology involving the leukocyte chemotaxis in the immune system<sup>5</sup> and progenitor cell migration during embryologic development of the cardiovascular,<sup>6,7</sup> hemopoietic,<sup>8</sup> and central nervous systems.<sup>9,10</sup> On the other hand, CXCR4 has also multiple functions in pathologic physiology. CXCR4 serves as a coreceptor for infection of T cell line-tropic (X4) strains of the human immunodeficiency virus type 1 (HIV-1<sup>a</sup>). Following activation of the gp120 subunits of the envelope glycoprotein by binding to CD4, CXCR4 leads to membrane

fusion and subsequent entry of the viral genome into the target cell.<sup>11,12</sup> Recently, Müller et al. disclosed that CXCL12/CXCR4 interactions participate in breast cancer metastasis analogous to programming directed migration in normal leukocytes and progenitor cells.<sup>13</sup> Expression of CXCR4 is enriched on the surface of malignant primary breast cancer cells while CXCL12 is preferentially expressed in organs that are frequent sites of metastasis in breast cancer, such as lung, liver, lymph nodes, and bone marrow. The coordinate actions between an attractant molecule and the corresponding receptor allow tumor cells to spread specifically to distant organs that provide a supportive niche. Furthermore, Nanki et al. reported that CXCL12/CXCR4 interactions might play a central role in memory T cell migration into inflamed rheumatoid arthritis (RA) synovium and for persisting inflammation at the affected site mediated by CD4<sup>+</sup> T cells.<sup>14</sup>

Thus, CXCR4 is considered as an important therapeutic target for multiple diseases. Several potent CXCR4 antagonists have been developed so far. Among them, a  $\beta$ -sheet-like 14-residue cyclic peptide **1** was identified by potency optimization of a 18-residue cyclic peptide isolated from horseshoe crabs (Figure 1).<sup>15</sup> The peptide **1** and its analogues were also characterized as HIV-1 entry inhibitors,<sup>16</sup> anticancer-metastatic,<sup>17,18</sup> and anti-RA agents.<sup>19</sup> Several other low-molecular-weight CXCR4 antagonists such as AMD3100<sup>20,21</sup> and KRH1636<sup>22</sup> have also been reported to inhibit HIV-1 infection through CXCR4. Recently, we have identified novel potent CXCR4 antagonists **2** and **3** by screening of two orthogonal cyclic pentapeptide libraries,<sup>23</sup> which were designed based on the structure–activity relationship studies on **1** (Figure 1).<sup>24</sup> These peptides contain two arginine, one 3-(2-naphthyl)alanine, and one tyrosine residue, that potentially

\* Corresponding author. Tel: +81-75-753-4551, Fax: +81-75-753-4570, E-mail: nfujii@pharm.kyoto-u.ac.jp

<sup>†</sup> Kyoto University.

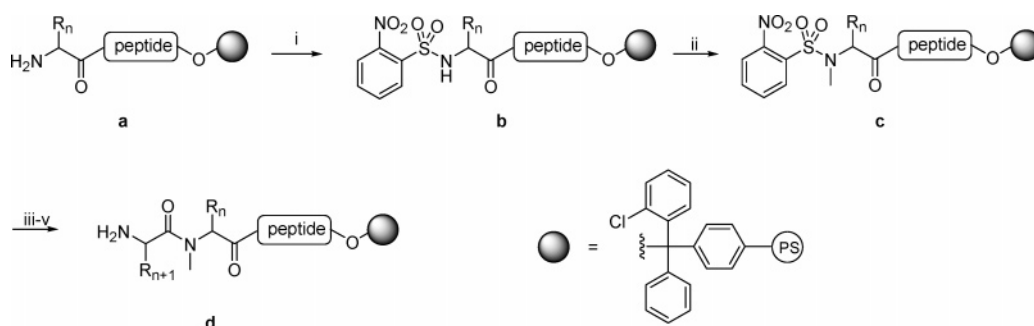
<sup>‡</sup> Medical College of Georgia.

<sup>§</sup> Tokyo Medical and Dental University.

<sup>||</sup> St. Marianna University.

<sup>§</sup> University of Louisville.

<sup>a</sup> Abbreviations: Nal, L-3-(2-naphthyl)alanine; Pic, pipercolic acid; Sar, sarcosine; HIV-1, human immunodeficiency virus type 1; RA, rheumatoid arthritis; SA-MD, simulated annealing molecular dynamics; AMD3100, 1,1'-[1,4-phenylenebis(methylene)]-bis(1,4,8,11-tetraazacyclotetradecane); KRH1636, *N*-{(S)-4-guanidino-1-[(S)-1-naphthalen-1-yl-ethylcarbamoyl]butyl}-4-[[pyridin-2-yl-methyl]amino]methyl]benzamide.

Scheme 1<sup>a</sup>

<sup>a</sup> Reagents: (i) *o*-nitrobenzenesulfonyl chloride, 2,4,6-collidine; (ii) MeOH, PPh<sub>3</sub>, DEAD; (iii) DBU, 2-mercaptoethanol; (iv) Fmoc-AA-OH, HATU, HOAT, DIPEA; (v) piperidine.

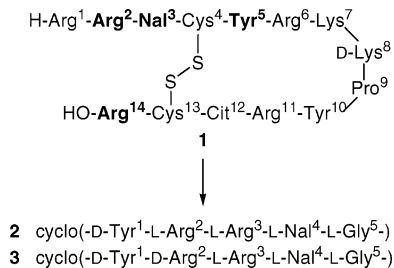


**Figure 1.** Structures of **1** and its downsized peptides **2** and **3**. Bold residues are the indispensable residues of **1** for the potent CXCR4-antagonistic activity. Nal = L-3-(2-naphthyl)alanine, Cit = L-citrulline.

correspond to the pharmacophore residues of the parent peptide **1**. We<sup>25–27</sup> and others<sup>28</sup> have performed several modifications on **2** including incorporation of (*E*)-alkene or reduced-amide dipeptide isosteres and conformationally constrained amino acid analogues, and fine-tuning of backbone ring structures. However, systematic modifications of **2** to design more potent antagonists have not been reported so far. In order to clarify the elements among the peptide side-chain and backbone functional groups indispensable for the ligand binding to CXCR4, chemical derivatization of **2** and **3** was conducted. In this manuscript, we describe the details of structure–activity relationship studies on cyclic pentapeptide-based CXCR4 antagonists **2** and **3** as well as identification of a more potent CXCR4 antagonist.

**Chemistry.** Synthesis on solid support of all peptides was performed on 2-chlorotrityl [(2-Cl)Trt] resin in parallel using usual Fmoc-based solid-phase peptide synthesis as described in the Experimental Section. *t*-Bu and 2,2,4,6,7-pentamethyl-dihydrobenzofuran-5-sulfonyl (Pbf) groups were employed for Tyr and Arg residue side-chain protection, respectively. L-Ala, D-Ala, L-Pro, D-Pro, L-pipecolic acid (L-Pic), D-Pic,  $\beta$ -alanine ( $\beta$ -Ala), and L-Nal were employed for the C-terminal residues of **12/19**, **13/20**, **14/21**, **15/22**, **16/23**, **17/24**, **18/25**, and **26/31**, respectively. The Gly residue was positioned at the C-terminal of the other peptide resins to avoid potential epimerization during the cyclization. For the preparation of *N*-methyl amino acid-containing peptide resins, an *N*-methyl group was incorporated on the  $\alpha$ -amino group by a site-selective method reported by Miller et al.<sup>29,30</sup> (Scheme 1). The  $\alpha$ -amino group was temporarily protected with an *o*-nitrobenzenesulfonyl (*o*-Ns) group before *N*-methylation by the Mitsunobu reaction. After removal of the *o*-Ns group by treatment with 1,8-diazabicyclo[5.4.0]undec-7-ene (DBU) and 2-mercaptoethanol, the subsequent amino acids were coupled using *O*-(7-azabenzotriazol-1-yl)-1,1,3,3-tetramethyluronium hexafluorophosphate (HATU)<sup>31</sup> as an activating reagent. Treatment of protected peptide resins with 20% (v/v) 1,1,1,3,3,3-hexafluoroisopropanol

**Table 1.** Biological Activities of **2**, **3**, and the Ala-Substituted Derivatives

peptide	sequence <sup>a</sup>	IC <sub>50</sub> ( $\mu$ M) <sup>b</sup>	EC <sub>50</sub> ( $\mu$ M) <sup>c</sup>
<b>2</b>	cyclo(-D-Tyr-L-Arg-L-Arg-L-Nal-Gly-)	0.004	0.16
<b>4</b>	cyclo(-D-Ala-L-Arg-L-Arg-L-Nal-Gly-)	> 1	115
<b>5</b>	cyclo(-D-Tyr-L-Ala-L-Arg-L-Nal-Gly-)	0.063	12
<b>6</b>	cyclo(-D-Tyr-L-Arg-L-Ala-L-Nal-Gly-)	> 1	> 120
<b>7</b>	cyclo(-D-Tyr-L-Arg-L-Arg-L-Ala-Gly-)	> 1	> 120
<b>3</b>	cyclo(-D-Tyr-D-Arg-L-Arg-L-Nal-Gly-)	0.008	0.39
<b>8</b>	cyclo(-D-Ala-D-Arg-L-Arg-L-Nal-Gly-)	0.13	29
<b>9</b>	cyclo(-D-Tyr-D-Ala-L-Arg-L-Nal-Gly-)	0.23	16
<b>10</b>	cyclo(-D-Tyr-D-Arg-L-Arg-L-Nal-Gly-)	> 1	60
<b>11</b>	cyclo(-D-Tyr-D-Arg-L-Arg-L-Ala-Gly-)	> 1	> 120

<sup>a</sup> The substituted residues from the parent peptides **2** and **3** are designated by underlining. <sup>b</sup> IC<sub>50</sub> values for the cyclic pentapeptides are based on inhibition of [<sup>125</sup>I]SDF-1 binding to CXCR4 transfectants of CHO cells. <sup>c</sup> EC<sub>50</sub> values are based on the inhibition of HIV-induced cytopathogenicity in MT-4 cells. All data are the mean values for at least three independent experiments.

(HFIP) in CH<sub>2</sub>Cl<sub>2</sub><sup>32</sup> provided linear protected peptides, which were cyclized with diphenylphosphoryl azide (DPPA) in DMF. Final deprotection with TFA–H<sub>2</sub>O (95:5) followed by reverse-phase HPLC purification afforded the cyclic peptides. All peptides were identified with ion-spray mass spectrometry, and the purity was more than 95% by analytical HPLC.

## Results and Discussion

**Identification of Indispensable Pharmacophore Functionality by Alanine-Scanning.** Our first attempt was to identify the minimal side-chain functional group requirement of **2** and **3** for CXCR4 antagonism. To evaluate the comparative significance of side-chain functionality, each residue except for the Gly residue of **2** and **3** was substituted with Ala. Because the chirality of Ala was identical to that of the corresponding residue in parent peptides, exhibition of similar conformations was expected even after the substitution. All Ala-substituted peptides **4–11** showed significantly less CXCR4 antagonistic and anti-HIV activities when compared to the parent peptides **2** and **3**. Ala<sup>3</sup>- or Ala<sup>4</sup>-substituted analogues **6**, **7**, **10**, and **11** did not show any CXCR4 antagonistic activity up to 1  $\mu$ M (Table 1). This indicates that all the side-chain functional groups are important for the high CXCR4 antagonistic activity. On the other hand, L/D-Ala<sup>2</sup>-substituted analogues, **5** and **9**, and D-Ala<sup>1</sup>-substituted analogue **8** maintained moderate activities (**5**: IC<sub>50</sub> = 63 nM, EC<sub>50</sub> = 12  $\mu$ M; **8**: IC<sub>50</sub> = 130 nM, EC<sub>50</sub> = 29  $\mu$ M; **9**: IC<sub>50</sub> = 230 nM, EC<sub>50</sub> = 16  $\mu$ M), although the potencies were less than one-twentieth of the parent peptides. These data suggest that the phenol group of D-Tyr<sup>1</sup> and a guanidino group of Arg<sup>2</sup> do not play a critical role in receptor binding, while guanidino group of Arg<sup>3</sup> and naphthalene group of Nal<sup>4</sup> are indispensable for the ligand interaction with CXCR4. This

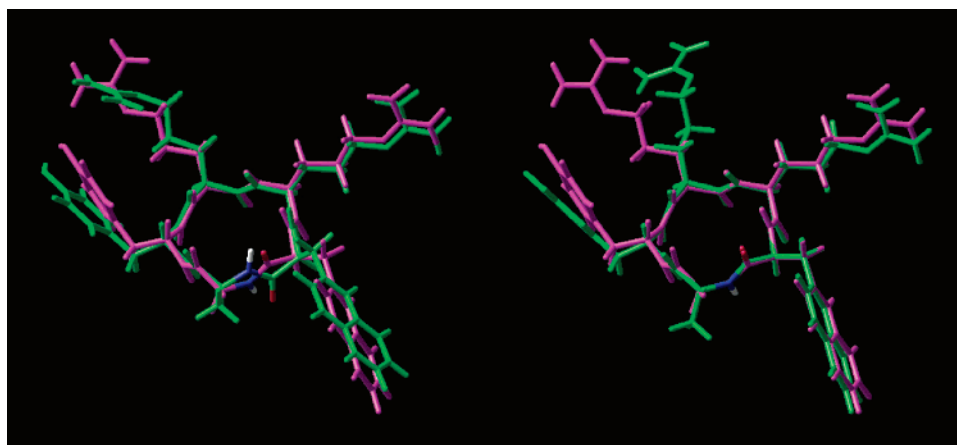


**Figure 2.** Superimposition of low-energy structures of **2** (purple) and **12** (green, left) or **13** (green, right).

propensity is consistent with the previous structure–activity relationship studies on **1**, where Ala-substitutions at the Arg<sup>2</sup>-Nal<sup>3</sup> motif in **1** were more sensitive to anti-HIV activity as compared to the substitution of the other important residues, such as Tyr<sup>5</sup> and Arg<sup>14</sup>.<sup>24</sup> It is noteworthy that two L/D-Ala<sup>2</sup>-substituted peptides **5** and **9** having opposite chiralities retained moderate bioactivities. Recently, we have shown that L-Arg<sup>2</sup> in **2** could be replaced by nonbasic amino acids such as L-Phe-(4-F) (L-4-fluorophenylalanine) and D-MeAla without significant loss of CXCR4 antagonistic activity.<sup>26,27</sup> Hence, the functional group or the spatial disposition of the Arg<sup>2</sup> guanidino group could be further optimized.

**Conformational Restriction of Cyclic Peptides by Modification of the Glycine Residue.** In contrast to the finding that all side-chain functional groups of **2** and **3** were important for the high CXCR4 antagonistic activities, the Gly<sup>5</sup> position had many possibilities for further optimization. Since the absence of a side chain in Gly<sup>5</sup> possibly affected the conformational flexibility of the peptide backbone, it was expected that use of chiral or conformationally constrained amino acids would potentially restrict the global conformations to decrease the entropy losses upon the peptide binding on CXCR4. In order to evaluate the structure–activity relationship at the Gly<sup>5</sup> position, simple aliphatic amino acids were utilized for this study. In our previous conformational studies on **2**, characteristic orientations of the amide carbonyl groups of D-Tyr,<sup>1</sup> Arg,<sup>2</sup> Arg,<sup>3</sup> and Gly<sup>5</sup> were observed in the low energy state.<sup>23</sup> These carbonyl oxygens were oriented away from the side chains of the respective following amino acids. This could be attributed to steric repulsion by a 1,3-allylic strain-like effect across the planar peptide bond.<sup>33</sup> On the other hand, the flexible Nal<sup>4</sup>  $\psi$  and Gly<sup>5</sup>  $\phi$  angles had been expected, since there were two possibilities of Nal<sup>4</sup> carbonyl oxygen orientation. However, the carbonyl oxygen was directed away from the Gly<sup>5</sup> pro-*R* hydrogen atom in the calculated conformations, while the other orientation was not exhibited. This implied that the incorporation of a side chain having *R*-chirality (D-amino acid) at the Gly<sup>5</sup> position could restrict the rotation of the Nal<sup>4</sup>-Gly<sup>5</sup> peptide bond plane. On the basis of this hypothesis, we introduced both enantiomers of Ala, Pro, and Pic to the Gly<sup>5</sup> position for conformational restriction. In addition,  $\beta$ -Ala was utilized for the optimization of carbon chain length at the Gly<sup>5</sup> position.

L-Ala<sup>5</sup>-substituted analogues **12** and **19** showed less than 10-fold lower CXCR4 antagonistic and anti-HIV activities of the parent peptides **2** and **3**, respectively (Table 2, **12**: IC<sub>50</sub> = 170 nM; EC<sub>50</sub> = 20  $\mu$ M, **19**: IC<sub>50</sub> = 92 nM; EC<sub>50</sub> = 10  $\mu$ M). By contrast and as expected, more than 8-fold higher potencies were

**Table 2.** Biological Activities of the Gly<sup>5</sup>-Modified Analogues of **2** and **3**

peptide	sequence <sup>a</sup>	IC <sub>50</sub> ( $\mu$ M) <sup>b</sup>	EC <sub>50</sub> ( $\mu$ M) <sup>c</sup>
<b>2</b>	cyclo(-D-Tyr-L-Arg-L-Arg-L-Nal-Gly-)	0.004	0.16
<b>12</b>	cyclo(-D-Tyr-L-Arg-L-Arg-L-Nal-L-Ala-)	0.17	20
<b>13</b>	cyclo(-D-Tyr-L-Arg-L-Arg-L-Nal-D-Ala-)	0.011	0.49
<b>14</b>	cyclo(-D-Tyr-L-Arg-L-Arg-L-Nal-D-Pro-)	> 1	- <sup>d</sup>
<b>15</b>	cyclo(-D-Tyr-L-Arg-L-Arg-L-Nal-D-Pro-)	> 1	- <sup>d</sup>
<b>16</b>	cyclo(-D-Tyr-L-Arg-L-Arg-L-Nal-L-Pic-)	> 1	- <sup>d</sup>
<b>17</b>	cyclo(-D-Tyr-L-Arg-L-Arg-L-Nal-D-Pic-)	> 1	- <sup>d</sup>
<b>18</b>	cyclo(-D-Tyr-L-Arg-L-Arg-L-Nal- $\beta$ -Ala-)	0.047	3.0
<b>3</b>	cyclo(-D-Tyr-D-Arg-L-Arg-L-Nal-Gly-)	0.008	0.37
<b>19</b>	cyclo(-D-Tyr-D-Arg-L-Arg-L-Nal-L-Ala-)	0.092	10
<b>20</b>	cyclo(-D-Tyr-D-Arg-L-Arg-L-Nal-D-Ala-)	0.011	0.67
<b>21</b>	cyclo(-D-Tyr-D-Arg-L-Arg-L-Nal-L-Pro-)	> 1	- <sup>d</sup>
<b>22</b>	cyclo(-D-Tyr-D-Arg-L-Arg-L-Nal-D-Pro-)	> 1	- <sup>d</sup>
<b>23</b>	cyclo(-D-Tyr-D-Arg-L-Arg-L-Nal-L-Pic-)	0.64	- <sup>d</sup>
<b>24</b>	cyclo(-D-Tyr-D-Arg-L-Arg-L-Nal-D-Pic-)	> 1	- <sup>d</sup>
<b>25</b>	cyclo(-D-Tyr-D-Arg-L-Arg-L-Nal- $\beta$ -Ala-)	0.35	38

<sup>a</sup> The substituted residues from the parent peptide **2** and **3** are underlined.

<sup>b</sup> IC<sub>50</sub> values for the cyclic pentapeptides are based on inhibition of [<sup>125</sup>I]SDF-1 binding to CXCR4 transfectants of CHO cells. <sup>c</sup> EC<sub>50</sub> values are based on the inhibition of HIV-induced cytopathogenicity in MT-4 cells.

<sup>d</sup> Not tested. All data are the mean values for at least three independent experiments.

observed for D-Ala<sup>5</sup>-substituted analogues **13** and **20** (**13**: IC<sub>50</sub> = 11 nM; EC<sub>50</sub> = 0.49  $\mu$ M, **20**: IC<sub>50</sub> = 11 nM; EC<sub>50</sub> = 0.67  $\mu$ M) as compared to the corresponding L-Ala<sup>5</sup>-substituted peptides **12** and **19**, respectively. The bioactivities of D-Ala<sup>5</sup>-substituted analogues were approximately half of the parent peptides **2** and **3**. This suggested that substitution with L-Ala<sup>5</sup> resulted in significant conformational change, while D-Ala<sup>5</sup> substitution kept the bioactive conformations of the parent peptides **2** and **3**. Simulated annealing molecular dynamics (SA-MD) analysis demonstrated that the backbone conformation of **13** was similar to that of **2** but different from that of **12** (Figure 2). Local conformations around Nal<sup>4</sup> and Gly<sup>5</sup>/D-Ala<sup>5</sup> were very similar between **2** and **13** as expected, while the conformation of L-Ala<sup>5</sup>-substituted analogues **12** differed particularly in the opposite orientation of the Nal<sup>4</sup> carbonyl oxygen. These calculated structures are consistent with the observed NOE data; in L-Ala<sup>5</sup>-substituted peptide **13**, strong NOE between Nal<sup>4</sup> H $\alpha$  and D-Ala<sup>5</sup> H<sup>N</sup> indicates that these hydrogen atoms were oriented into the same direction. On the other hand, the observed weak NOE between Nal<sup>4</sup> H $\alpha$  and L-Ala<sup>5</sup> H<sup>N</sup> in peptide **12** indicates these hydrogen atoms were oriented into the opposite directions. The 1,3-pseudo allylic strain between the Nal<sup>4</sup> carbonyl oxygen and the  $\alpha$ -methyl group of D/L-Ala<sup>5</sup> could result in these different conformational preferences between **12** and **13**. This

**Table 3.** Biological Activities of *N*-Methyl Amino Acid-Containing Analogues of **2** and **3**

peptide	sequence <sup>a</sup>	IC <sub>50</sub> ( $\mu$ M) <sup>b</sup>	EC <sub>50</sub> ( $\mu$ M) <sup>c</sup>
<b>2</b>	cyclo(-D-Tyr-L-Arg-L-Arg-L-Nal-Gly-)	0.004	0.16
<b>26</b>	cyclo(-D-MeTyr-L-Arg-L-Arg-L-Nal-Gly-)	0.128	- <sup>d</sup>
<b>27</b>	cyclo(-D-Tyr-L-MeArg-L-Arg-L-Nal-Gly-)	0.023	1.399
<b>28</b>	cyclo(-D-Tyr-L-Arg-L-MeArg-L-Nal-Gly-)	0.099	9.534
<b>29</b>	cyclo(-D-Tyr-L-Arg-L-Arg-L-MeNal-Gly-)	0.250	- <sup>d</sup>
<b>30</b>	cyclo(-D-Tyr-L-Arg-L-Arg-L-Ala-Sar-)	0.167	- <sup>d</sup>
<b>3</b>	cyclo(-D-Tyr-D-Arg-L-Arg-L-Nal-Gly-)	0.008	0.39
<b>31</b>	cyclo(-D-MeTyr-D-Arg-L-Arg-L-Nal-Gly-)	0.157	- <sup>d</sup>
<b>32</b>	cyclo(-D-Tyr-D-MeArg-L-Arg-L-Nal-Gly-)	0.003	0.088
<b>33</b>	cyclo(-D-Tyr-D-Arg-L-MeArg-L-Nal-Gly-)	0.021	0.782
<b>34</b>	cyclo(-D-Tyr-D-Arg-L-Arg-L-MeNal-Gly-)	0.563	- <sup>d</sup>
<b>35</b>	cyclo(-D-Tyr-D-Arg-L-Arg-L-Nal-Sar-)	0.256	- <sup>d</sup>

<sup>a</sup> *N*-Methylated residues are underlined. <sup>b</sup> IC<sub>50</sub> values for the cyclic pentapeptides are based on inhibition of [<sup>125</sup>I]SDF-1 binding to CXCR4 transfectants of CHO cells. <sup>c</sup> EC<sub>50</sub> values are based on the inhibition of HIV-induced cytopathogenicity in MT-4 cells. <sup>d</sup> Not tested. All data are the mean values for at least three independent experiments.

could explain the reason for the higher potencies of D-Ala<sup>5</sup>-substituted analogues. The above information could serve for the further optimization of the Gly<sup>5</sup> position using D-amino acids having side-chain functionality.

Our next approach was to restrict global conformations of peptides **2** and **3** using cyclic amino acids such as L/D-Pro and L/D-Pic. These amino acids can provide a fused ring structure of cyclic peptides consisting of small and large rings. It was expected that the limited  $\phi$  angle flexibility of Pro and Pic could contribute to the global conformational restriction.<sup>34</sup> Covalent linkage between the amide nitrogen and the side chain could also produce a favorable orientation of the Nal<sup>4</sup> carbonyl oxygen. However, L/D-Pro<sup>5</sup>- and L/D-Pic<sup>5</sup>-substituted peptides **14**–**17**, **21**, **22**, and **24** did not show CXCR4 inhibitory activities with IC<sub>50</sub> values lower than 1  $\mu$ M. Even the most potent peptide **23** exhibited an IC<sub>50</sub> of only 0.64  $\mu$ M. This suggests that the presence of cyclic amino acids at this position is sterically or conformationally unfavorable for the peptide–CXCR4 interaction. We could also assume that an amide proton at this position is required for high activity. This was supported by the fact that peptides having a sarcosin (Sar) at the Gly<sup>5</sup> position possessed less than one-thirtieth CXCR4 antagonistic activity of the parent peptides (see the next section).  $\beta$ -Ala<sup>5</sup>-substituted analogues **18** and **25** showed lower CXCR4 antagonistic and anti-HIV activities (**18**: IC<sub>50</sub> = 47 nM, EC<sub>50</sub> = 3  $\mu$ M; **25**: IC<sub>50</sub> = 350 nM, EC<sub>50</sub> = 38  $\mu$ M), indicating that expansion of the backbone ring size (16-membered ring) at this position is not favorable. Recently, we showed that reduction in the size of the backbone ring using  $\gamma$ -Nal [4-amino-5-(2-naphthyl)pentanoic acid] or  $\gamma$ -(*E*)-Nal [(*E*)-4-amino-5-(2-naphthyl)pent-2-enoic acid] unit (14-membered ring) instead of Nal<sup>4</sup>-Gly<sup>5</sup> dipeptide resulted in moderate to significant loss of CXCR4 antagonistic activity.<sup>27</sup> These observations suggest the importance of Gly<sup>5</sup> as a spacer for appropriate spatial orientation of the CXCR4 antagonist pharmacophores.

**Identification of a Novel Potent CXCR4 Antagonist through *N*-Methyl Amino Acid-Scanning of **2** and **3**.** *N*-Methylation of the peptide backbone has been shown to be a valuable method in structure–activity relationship studies on bioactive peptides.<sup>35–37</sup> Substitutions with *N*-methyl amino acids often cause an increase or decrease in potency and selectivity of peptide ligands, providing useful information on the bioactive conformation. Hence, every amide bond of **2** and **3** was replaced sequentially with the corresponding *N*-methylated amide, and the bioactivities of obtained peptides were evaluated (Table 3).

Peptides **26**, **28**, **29**, and **30** derived from *N*-methyl amino acid-scanning of peptide **2** showed more than 25-fold less CXCR4 antagonistic activity as compared to the parent peptide **2**. *N*-Methylated analogues **31**, **34**, and **35** also showed a significant decrease in CXCR4 antagonism as compared to the parent peptide **3**. Use of L-MeArg<sup>3</sup> in peptide **33** slightly decreased the activity. *N*-Methylation at the Nal<sup>4</sup> position caused a remarkable decrease in CXCR4 antagonistic activity (**29**: IC<sub>50</sub> = 250 nM; **34**: IC<sub>50</sub> = 563 nM), suggesting that *N*-methylation at the putative receptor-binding motif (Arg<sup>3</sup>-Nal<sup>4</sup>) is unfavorable probably due to the absence of an amide proton. Previously, we showed that replacement of the Arg<sup>3</sup>-Nal<sup>4</sup> motif with the corresponding (*E*)-alkene dipeptide isostere unit (L-Arg<sup>3</sup>- $\psi$ [(*E*)-CH=CH]-L-Nal<sup>4</sup>) or a reduced amide isostere unit (L-Arg<sup>3</sup>- $\psi$ -[CH<sub>2</sub>-NH]-L-Nal<sup>4</sup>) caused a significant loss of CXCR4 antagonistic activity.<sup>25</sup> These observations also indicate the importance of the Arg<sup>3</sup>-Nal<sup>4</sup> amide bond in both functional and conformational aspects.

On the other hand, the L/D-MeArg<sup>2</sup>-substituted peptides **27** and **32** showed potent CXCR4 antagonistic and anti-HIV activities (**27**: IC<sub>50</sub> = 23 nM, EC<sub>50</sub> = 1.4  $\mu$ M; **32**: IC<sub>50</sub> = 3.0 nM, EC<sub>50</sub> = 0.088  $\mu$ M), indicating that *N*-methylation at Arg<sup>2</sup> is not critical to antagonist activity. Interestingly, the D-MeArg<sup>2</sup> substitution (**32**) led to approximately 2-fold increase of CXCR4 antagonistic activity and more than 40-fold anti-HIV activity as compared with **3**, and these activities were nearly equal to those of **2**. NMR and SA-MD calculations showed that major conformer of **32** exhibited a backbone conformation similar to **2** but different from the parent peptide **3**, particularly with respect to the orientation of D-Tyr<sup>1</sup> carbonyl oxygen (Figure 3).<sup>38</sup> This conformation was also supported by strong NOEs between [D-Arg<sup>2</sup> H $\alpha$  and D-Arg<sup>2</sup> H<sup>NMe</sup>] and [D-Arg<sup>2</sup> H<sup>NMe</sup> and Arg<sup>3</sup> H<sup>N</sup>] in **32** (the corresponding strong NOEs were not observed in the parent peptide **3**; see Supporting Information). It is possible that an unfavorable 1,3-pseudo-allylic strain-like effect between the *N*-methyl group of D-MeArg<sup>2</sup> and D-Tyr<sup>1</sup> side chain of **32** induced the flip of D-Tyr<sup>1</sup>-D-Arg<sup>2</sup> amide group upon *N*-methylation of D-Arg<sup>2</sup>, resulting in the identical local conformation around the D-Tyr<sup>1</sup>-D-MeArg<sup>2</sup> dipeptide with the D-Tyr<sup>1</sup>-L-Arg<sup>2</sup> conformation of **2**. Previously, we have shown a similar local conformational change upon *N*-methylation at the same position in D-Ala<sup>2</sup>-substituted analogues of **2**; i.e. cyclo(-D-Tyr<sup>1</sup>-D-MeAla<sup>2</sup>-Arg<sup>3</sup>-Nal<sup>4</sup>-Gly<sup>5</sup>-) showed 5-fold higher CXCR4 antagonistic activity (IC<sub>50</sub> = 42 nM) than the nonmethylated peptide, cyclo(-D-Tyr<sup>1</sup>-D-Ala<sup>2</sup>-Arg<sup>3</sup>-Nal<sup>4</sup>-Gly<sup>5</sup>-) **9**.<sup>27</sup> It is also noted that the lower bioactivities of peptide **27** compared to **2** could be explained by the potential flip of the D-Tyr<sup>1</sup>-L-MeArg<sup>2</sup> amide bond orientation by *N*-methylation. These data suggest that the amide proton of Arg<sup>2</sup> has little contribution to bioactivity, and the amide bond orientation between D-Tyr<sup>1</sup> and D-MeArg<sup>2</sup> in **32** may contribute to its enhanced biological function.

## Conclusion

Our present Ala-scanning study has shown that all of the side-chain functional groups contribute to high CXCR4 antagonistic activity of peptides **2** and **3**. In particular, Arg<sup>3</sup> and Nal<sup>4</sup> were proven to be indispensable for CXCR4 antagonistic activity. We have also shown that L-Ala substitution for Gly<sup>5</sup> of **2** or **3** caused a remarkable decrease in CXCR4 antagonistic and anti-HIV activities, while D-Ala substitution retained activity. Conformational studies revealed that D-Ala-substituted analogue **13** adopted a backbone conformation similar to that of **2**, which allows the rationalization of the biological activity for these

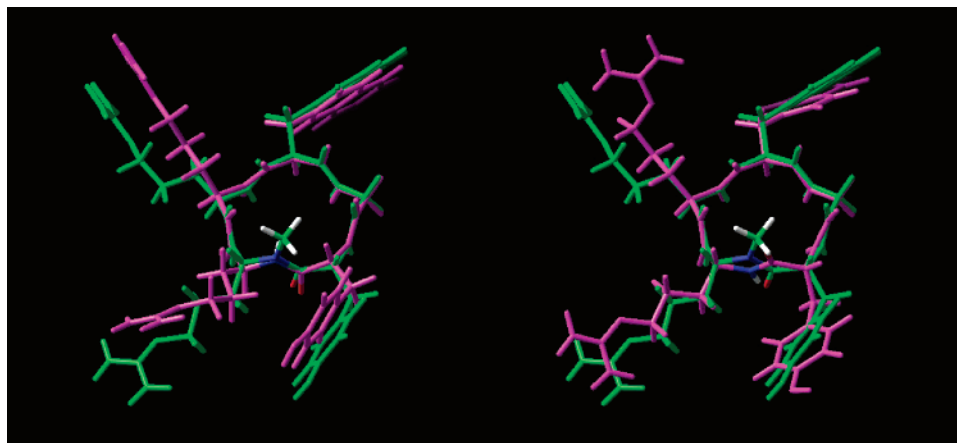


**Figure 3.** Superimposition of low-energy structures of **32** (green) and **2** (purple, left) or **3** (purple, right).

series of analogues. In addition, through comprehensive *N*-methyl-scanning of all residues in **2** and **3**, the *N*-methylated analogue **32** was characterized as one of the most potent cyclic pentapeptide-based CXCR4 antagonists synthesized thus far. The slight increase in CXCR4 antagonistic activity in **32** as compared to its nonmethylated analogue **3** could be explained by the favorable peptide bond orientation at the *N*-methylation site. Conformational studies suggested that the high potency in these series of compounds is due to the orientation of the backbone amide bonds, although direct interaction of the amide functions with the CXCR4 receptor is not clear. These results give valuable insight for understanding the ligand–receptor interactions and may also provide useful approaches for the design of new low-molecular-weight CXCR4 antagonists.

### Experimental Section

**General.** Exact mass (HRMS) spectra were recorded on a JEOL JMS-01SG-2 or JMS-HX/HX 110A mass spectrometer. The ion-spray mass spectrum was obtained with a Sciex APIIII triple quadrupole mass spectrometer (Toronto, Canada). Optical rotations were measured in water or 50% (v/v) water/AcOH solution with a Horiba high-sensitive polarimeter SEPA-200. <sup>1</sup>H NMR spectra were recorded using a Bruker AM 600 or JEOL JNM-ECA600 spectrometer at 600 MHz frequency, or JEOL JNM-AL400 spectrometer at 400 MHz frequency. Chemical shifts are calibrated to the solvent signal (2.49 ppm for DMSO, or 4.65 ppm for H<sub>2</sub>O; s = singlet, d = doublet, dd = double doublet, m = multiplet). For HPLC separations, a Cosmosil 5C18-ARII analytical column (Nacalai Tesque, 4.6 × 250 mm, flow rate 1 mL/min) or a Cosmosil 5C18-ARII preparative column (Nacalai Tesque, 20 × 250 mm, flow rate 11 mL/min) was employed, and eluting products were detected by UV at 220 nm. A solvent system consisting of 0.1% TFA in water (v/v, solvent A) and 0.1% TFA in MeCN (v/v, solvent B) was used for HPLC elution.

**Preparation of Amino Acid-Loaded 2-Chlorotrityl Resin.** 2-Chlorotrityl chloride resin (1.25 mmol/g, 0.63 mmol) was treated with Fmoc-amino acid (0.69 mmol) and *N,N*-diisopropylethylamine (DIPEA) (2.77 mmol) in CH<sub>2</sub>Cl<sub>2</sub> (5.00 mL) for 1.5 h. After the resin was washed with CH<sub>2</sub>Cl<sub>2</sub>, it was dried in vacuo. The loading was determined by measuring at 290 nm UV absorption of the piperidine-treated sample: Fmoc-L-Nal-(2-Cl)Trt-resin (0.72 mmol/g); Fmoc-L-Pro-(2-Cl)Trt-resin (0.78 mmol/g); Fmoc-D-Pro-(2-Cl)Trt-resin (0.81 mmol/g); Fmoc-L-Pic-(2-Cl)Trt-resin (0.88 mmol/g); Fmoc-D-Pic-(2-Cl)Trt-resin (0.84 mmol/g); Fmoc-β-Ala-(2-Cl)Trt-resin (0.79 mmol/g).

**Fmoc-Based Solid-Phase Peptide Synthesis.** Protected peptide resins were manually constructed on a 0.10 mmol scale on H-L-Ala-(2-Cl)Trt-resin (0.89 mmol/g) for **12** and **19**, H-D-Ala-(2-Cl)Trt-resin (0.90 mmol/g) for **13** and **20**, Fmoc-L-Pro-(2-Cl)Trt-resin for **14** and **21**, Fmoc-D-Pro-(2-Cl)Trt-resin for **15** and **22**, Fmoc-

L-Pic-(2-Cl)Trt-resin for **16** and **23**, Fmoc-D-Pic-(2-Cl)Trt-resin for **17** and **24**, Fmoc-β-Ala-(2-Cl)Trt-resin for **18** and **25**, Fmoc-L-Nal-(2-Cl)Trt-resin for **26** and **31**, and H-Gly-Trt(2-Cl)Trt-resin (0.75 mmol/g) for the other peptides. Fmoc-amino acids were coupled using 1,3-diisopropylcarbodiimide (DIPCDI, 0.078 mL, 0.50 mmol) and *N*-hydroxybenzotriazole hydrate (HOBT·H<sub>2</sub>O, 76 mg, 0.50 mmol) in DMF (1.0 mL) for 1.5 h. For the coupling of Fmoc-amino acid to the *N*-methyl amino acid, HATU (186 mg, 0.49 mmol) and 1-hydroxy-7-azabenzotriazole (HOAt, 68 mg, 0.50 mmol) were employed in place of DIPCDI/HOBT. The Fmoc group was deprotected by treatment with 20% (v/v) piperidine–DMF for 20 min.

***N*-Methyl Modification of *N*-Terminal α-Amino Group on Resin.** Resin (0.10 mmol) was treated with *o*-nitrobenzenesulfonyl chloride (66.5 mg, 0.30 mmol) and 2,4,6-collidine (0.066 mL, 0.50 mmol) in CH<sub>2</sub>Cl<sub>2</sub> (1.0 mL) for 2 h at room temperature. After the resin was washed (CH<sub>2</sub>Cl<sub>2</sub> × 3, DMF × 3, and THF × 3), to a suspension of the *N*-Ns-protected resin in anhydrous THF (1.0 mL) were added MeOH (0.020 mL, 0.50 mmol), PPh<sub>3</sub> (131 mg, 0.50 mmol), and diethyl diazodicarboxylate (0.227 mL, 0.50 mmol) at 0 °C. The mixture was shaken for 2 h at room temperature, followed by washing the resin (THF × 3 and CHCl<sub>3</sub> × 3). The *N*-methylated resin was treated with DBU (0.075 mL, 0.50 mmol) and 2-mercaptoethanol (0.070 mL, 1.0 mmol) for 1.5 h at room temperature to give the protected peptide resin having an *N*-methyl amino acid at the *N*-terminus.

**Cleavage of Protected Peptides from the Resin and Cyclization.** Protected peptide resin was treated with 20% (v/v) HFIP–CH<sub>2</sub>Cl<sub>2</sub> (10 mL) for 2 h. After filtration of the resin, the filtrate was concentrated to provide the crude linear protected peptide. To the solution of the residue in DMF (30 mL) were added DPPA (0.539 mL, 0.25 mmol) and NaHCO<sub>3</sub> (42.0 mg, 0.50 mmol) at –40 °C. After being stirred for 36 h at room temperature, the whole was filtered, and the filtrate was concentrated to give the protected cyclic peptide, which was subjected to solid-phase extraction (SPE) over basic alumina in CHCl<sub>3</sub>–MeOH (9:1) to remove inorganic salts derived from DPPA.

**Deprotection of Protected Cyclic Peptide and HPLC purification.** Protected cyclic peptides were treated with 95% (v/v) TFA solution (10 mL) for 2 h at room temperature. Concentration under reduced pressure and purification by preparative HPLC gave cyclic peptides.

**Cell Culture.** Human T-cell lines, MT-4 and MOLT-4 cells were grown in RPMI 1640 medium containing 10% heat-inactivated fetal calf serum, 100 IU/mL penicillin, and 100 μg/mL streptomycin.

**Virus.** A strain of X4-HIV-1, HIV-1IIB, was used for the anti-HIV assay. This virus was obtained from the culture supernatant of HIV-1 persistently infected MOLT-4/HIVIIB cells and stored at –80 °C until used.

**Anti-HIV-1 Assay.** Anti-HIV-1 activity was determined based on the protection against HIV-1-induced cytopathogenicity in MT-4

cells. Various concentrations of test compounds were added to HIV-1 infected MT-4 cells at multiplicity of infection (MOI) of 0.01 and placed in wells of a flat-bottomed microtiter tray ( $1.5 \times 10^4$  cells/well). After 5 days incubation at 37 °C in a CO<sub>2</sub> incubator, the number of viable cells was determined using the 3-(4,5-dimethylthiazol-2-yl)-2,5-diphenyltetrazolium bromide (MTT).

**[<sup>125</sup>I]-SDF-1 Binding and Displacement.** Stable CHO cell transfectants expressing CXCR4 variant were prepared as describe previously.<sup>39</sup> CHO transfectants were harvested by treatment with trypsin-EDTA, allowed to recover in complete growth medium (MEM- $\alpha$ , 100  $\mu$ g/mL penicillin, 100  $\mu$ g/mL streptomycin, 0.25  $\mu$ g/mL amphotericin B, 10% (v/v)) for 4–5 h, and then washed in cold binding buffer (PBS containing 2 mg/mL BSA). For ligand binding, the cells were resuspended in binding buffer at  $1 \times 10^7$  cell/mL, and 100  $\mu$ L aliquots were incubated with 0.1 nM of [<sup>125</sup>I]-SDF-1 (Perkin-Elmer Life Sciences) for 2 h on ice under constant agitation. Free and bound radioactivities were separated by centrifugation of the cells through an oil cushion, and bound radioactivity was measured with gamma-counter (Cobra, Packard, Downers Grove, IL). Inhibitory activity of test compounds was determined based on the inhibition of [<sup>125</sup>I]-SDF-1 binding to CXCR4 transfectants (IC<sub>50</sub>).

**NMR Spectroscopy.** The peptide sample was dissolved in DMSO-*d*<sub>6</sub> at a concentration of 5 mM. <sup>1</sup>H NMR spectra of the peptides were recorded at 300 K. The assignment of the proton resonance was achieved by use of <sup>1</sup>H–<sup>1</sup>H COSY spectra. <sup>3</sup>J(H<sup>N</sup>, H <sup>$\alpha$</sup> ) coupling constants were measured from one-dimensional spectra. The mixing time for NOESY experiments was set at 200 ms. NOESY spectra were composed of 512 real points in the F2 dimension and 256 real points, which were zero-filled to 256 points in the F1 dimension, with 144 scans per t1 increment. The cross-peak intensities were evaluated by relative build-up rates of the cross-peaks. **2**, **3**, **12**, and **13** exhibited one set of signals in <sup>1</sup>H NMR spectra. On the other hand, two distinct sets of signals were observed in <sup>1</sup>H NMR spectra of **32** with relative populations of 69% and 31%, indicating the existence of two conformations. For the minor conformer, NOESY spectra showed the NOE contact between  $\alpha$  protons of D-Tyr<sup>1</sup> and D-MeArg<sup>2</sup> which is characteristic of the amide bond in a *cis* conformation. The major conformer did not exhibit any sequential H <sup>$\alpha$</sup> –H <sup>$\alpha$</sup>  NOEs, suggesting this conformer adopt an all-*trans* conformation. The calculated structures of major and minor conformers exhibited *trans*- and *cis*-D-Tyr<sup>1</sup>-D-MeArg<sup>2</sup> amide bond, respectively, which was consistent with the observed NOEs.

**Calculation of Structures.** The structure calculations were performed on a Silicon Graphics Origin 2000 workstation with the NMR refine program within the Insight II/Discover package using the consistent valence force field (CVFF). Pseudoatoms were defined for the CH<sub>3</sub> <sup>$\alpha$</sup>  protons of L-Ala<sup>5</sup> of **12**, D-Ala<sup>5</sup> of **13**, and *N*-methyl protons of **32**, and for all methylene protons of Nal<sup>4</sup>, D-Tyr<sup>1</sup>, D/L-Arg<sup>2</sup>, and Arg<sup>3</sup>, prochirality of which were not identified from <sup>1</sup>H NMR data. The dihedral  $\phi$  angle constraints were calculated based on the Karplus equation:  $^3J(\text{H}^{\text{N}}, \text{H}^{\alpha}) = 6.7 \cos^2(\theta - 60^\circ) - 1.3 \cos(\theta - 60^\circ) + 1.5$ . Lower and upper angle errors were set to 15°. The NOESY spectrum with a mixing time of 200 ms was used for the estimation of the distances restraints between protons. The NOE intensities were classified into three categories (strong, medium, and weak) based on the number of contour lines in the cross-peaks to define the upper-limit distance restraints (1.7, 3.5, and 5.0 Å, respectively). The upper-limit restraints were increased by 1.0 Å for the involved pseudoatoms. Lower bounds between nonbonded atoms were set to their van der Waals radii (1.8 Å). These distance and dihedral angle restraints were included with force constants of 25–100 kcal/mol·Å<sup>2</sup> and 25–100 kcal/mol·rad<sup>2</sup>, respectively. The 50 initial structures generated by the NMR refine program randomly were subjected to the simulated annealing calculations. The final minimization stage was achieved until the maximum derivative became less than 0.01 kcal/mol·Å<sup>2</sup> by the steepest descents and conjugate gradients methods. Excellent convergence was seen in the backbone structure of all calculated

structures. The root-mean-square deviation (rmsd) values for all backbone structures of ten low-energy structures were below 0.23 Å.

**Acknowledgment.** This work was supported by Grant-in-Aid for Scientific Research from the Ministry of Education, Culture, Sports, Science, and Technology of Japan, and Health and Labour Sciences Research Grants (Research on HIV/AIDS) and Philip Morris USA Inc. and Philip Morris International. Computation time was provided by the Supercomputer Laboratory, Institute for Chemical Research, Kyoto University. S.U. and S.O. are grateful for the JSPS Research Fellowships for Young Scientists.

**Supporting Information Available:** Characterization data for all new compounds, <sup>1</sup>H NMR data of **2**, **3**, **12**, **13**, and **32**, and HPLC charts of representative compounds. This material is available free of charge via the Internet at <http://pubs.acs.org>.

## References

- (1) Murphy, P. M.; Baggiolini, M.; Charo I. F.; Herbert, C. A.; Horuk, R.; Matsushima, K.; Miller, L. H.; Oppenheim, J. J.; Power, C. A. International union of pharmacology. XXII. Nomenclature for chemokine receptors. *Pharmacol. Rev.* **2000**, *52*, 145–176.
- (2) Mackay, C. R.; Chemokines: immunology's high impact factors. *Nat. Immunol.* **2001**, *2*, 95–101.
- (3) Premack, B. A.; Schall, T. J. Chemokine receptors: gateways to inflammation and infection. *Nat. Med.* **1996**, *2*, 1174–1178.
- (4) Zlotnik, K.; Yoshie, O. Chemokines: a new classification system and their role in immunity. *Immunity* **2000**, *12*, 121–127.
- (5) Bleul, C. C.; Fuhlbrigge, R. C.; Casanovas, J. M.; Aiuti, A.; Springer, T. A. A highly efficacious lymphocyte chemoattractant, stromal cell-derived factor 1 (SDF-1). *J. Exp. Med.* **1996**, *2*, 1101–1109.
- (6) Tachibana, K.; Hirota, S.; Iizasa, H.; Yoshida, H.; Kawabata, K.; Kataoka, Y.; Kitamura, Y.; Matsushima, K.; Yoshida, N.; Nishikawa, S.; Kishimoto, T.; Nagasawa, T. The chemokine receptor CXCR4 is essential for vascularization of the gastrointestinal tract. *Nature* **1998**, *393*, 591–594.
- (7) Nagasawa, T.; Hirota, S.; Tachibana, K.; Takakura, N.; Nishikawa, S.; Kitamura, Y.; Yoshida, N.; Kikutani, H.; Kishimoto, T. Defects of B-cell lymphopoiesis and bone-marrow myelopoiesis in mice lacking the CXC chemokine PBSF/SDF-1. *Nature* **1996**, *382*, 635–638.
- (8) Aiuti, A.; Webb, I. J.; Bleul, C.; Springer, T.; Gutierrez-Ramos, J. C. The chemokine SDF-1 is a chemoattractant for human CD34<sup>+</sup> hematopoietic progenitor cells and provides a new mechanism to explain the mobilization of CD34<sup>+</sup> progenitors to peripheral blood. *J. Exp. Med.* **1997**, *2*, 111–120.
- (9) Zhu, Y.; Yu, Y.; Zhang, X. C.; Nagasawa, T.; Wu, J. Y.; Rao, Y. Role of the chemokine SDF-1 as the meningeal attractant for embryonic cerebellar neurons. *Nat. Neurosci.* **2002**, *5*, 719–720.
- (10) Stumm, R. K.; Zhou, C.; Ara, T.; Lazarini, F.; Dubois-Dalq, M.; Nagasawa, T.; Holt, V.; Schulz, S. CXCR4 regulates interneuron migration in the developing neocortex. *J. Neurosci.* **2003**, *23*, 5123–5130.
- (11) Feng, Y.; Broder, C. C.; Kennedy, P. E.; Berger, E. A. HIV-1 entry co-factor: Functional cDNA cloning of a seven-transmembrane G protein-coupled receptor. *Science* **1996**, *272*, 872–877.
- (12) Oberlin, E.; Amara, A.; Bachelier, F.; Bessia, C.; Virelizier, J. L.; Arenzana-Seisdedos, F.; Schwartz, O.; Heard, J. M.; Clark-Lewis, I.; Legler, D. L.; Loetscher, M.; Baggiolini, M.; Moser, B. The CXC chemokine SDF-1 is the ligand for LESTR/fusin and prevents infection by T-cell-line-adapted HIV-1. *Nature* **1996**, *382*, 833–835.
- (13) Müller, A.; Homey, B.; Soto, H.; Ge, N.; Catron, D.; Buchanan, M. E.; McClanahan, T.; Murphy, E.; Yuan, W.; Wagner, S. M.; Barrera, J. L.; Mohar, A.; Verástegui, E.; Zlotnik, A. Involvement of chemokine receptors in breast cancer metastasis. *Nature* **2001**, *410*, 50–56.
- (14) Nanki, T.; Hayashida, K.; El-Gabalawy, H. S.; Suson, S.; Shi, K.; Girschick, H. J.; Yavuz, S.; Lipsky, P. E. Stromal cell-derived factor-1-CXC chemokine receptor interactions play a central role in CD4<sup>+</sup> T cell accumulation in rheumatoid arthritis synovium. *J. Immunol.* **2000**, *165*, 6590–6598.
- (15) Masuda, M.; Nakashima, H.; Ueda, T.; Naba, H.; Ikoma, R.; Otaka, A.; Terakawa, Y.; Tamamura, H.; Ibuka, T.; Murakami, T.; Koyanagi, Y.; Waki, M.; Matsumoto, A.; Yamamoto, N.; Funakoshi, S.; Fujii,

- N. A novel anti-HIV synthetic peptide, T-22 ([Tyr<sup>5,12</sup>,Lys<sup>7</sup>]-polyphemus II). *Biochem. Biophys. Res. Commun.* **1992**, *189*, 845–850.
- (16) Tamamura, H.; Xu, Y.; Hattori, T.; Zhang, X.; Arakaki, R.; Kanbara, K.; Omagari, A.; Otaka, A.; Ibuka, T.; Yamamoto, N.; Nakashima, H.; Fujii, N. A low molecular weight inhibitor against the chemokine receptor CXCR4: a strong anti-HIV peptide T140. *Biochem. Biophys. Res. Commun.* **1998**, *253*, 877–882.
- (17) Tamamura, H.; Hori, A.; Kanzaki, N.; Hiramatsu, K.; Mizumoto, M.; Nakashima, H.; Yamamoto, N.; Otaka, A.; Fujii, N. T140 analogues as CXCR4 antagonists identified as anti-metastatic agent in the treatment of breast cancer. *FEBS Lett.* **2003**, *550*, 79–83.
- (18) Takenaga, M.; Tamamura, H.; Hiramatsu, K.; Nakamura, N.; Yamaguchi, Y.; Kitagawa, A.; Kawai, S.; Nakashima, H.; Fujii, N.; Igarashi, R. A single treatment with microcapsules containing a CXCR4 antagonist suppressed pulmonary metastasis of murine melanoma. *Biochem. Biophys. Res. Commun.* **2004**, *320*, 226–232.
- (19) Tamamura, H.; Fujisawa, M.; Hiramatsu, K.; Mizumoto, M.; Nakashima, H.; Yamamoto, N.; Otaka, A.; Fujii, N. Identification of a CXCR4 antagonist, T140 analog, as anti-rheumatoid arthritis agent. *FEBS Lett.* **2004**, *569*, 99–104.
- (20) Schols, D.; Struyf, S.; Van Damme, J.; Este, J. A.; Henson, G.; De Clercq, E. Inhibition of T-tropic HIV strains by selective antagonization of the chemokine receptor CXCR4. *J. Exp. Med.* **1997**, *186*, 1383–1388.
- (21) Donzella, G. A.; Schols, D.; Lin, S. W.; Este, J. A.; Nagashima, K. A.; Maddon P. J. AMD3100, a small molecule inhibitor of HIV-1 entry via the CXCR4 co-receptor. *Nat. Med.* **1998**, *4*, 72–76.
- (22) Ichiya, K.; Yokoyama-Kumakura, S.; Tanaka, Y.; Tanaka, R.; Hirose, K.; Bannai, K.; Edamatsu, T.; Yanaka, M.; Niitani, Y.; Miyano-Kurosaki, N.; Takaku, H.; Koyanagi, Y.; Yamamoto, N. A duodenally absorbable CXC chemokine receptor 4 antagonist, KRH-1636, exhibits a potent and selective anti-HIV-1 activity. *Proc. Natl. Acad. Sci. U.S.A.* **2003**, *100*, 4185–4190.
- (23) Fujii, N.; Oishi, S.; Hiramatsu, K.; Araki, T.; Ueda, S.; Tamamura, H.; Otaka, A.; Kusano, S.; Terakubo, S.; Nakashima, H.; Broach, J. A.; Trent, J. O.; Wang, Z.; Peiper, S. C. Molecular-size reduction of a potent CXCR4-chemokine antagonist using orthogonal combination of conformation- and sequence-based libraries. *Angew. Chem. Int. Ed.* **2003**, *42*, 3251–3253.
- (24) Tamamura, H.; Omagari, A.; Oishi, S.; Kanamoto, T.; Yamamoto, N.; Peiper, S. C.; Nakashima, H.; Otaka, A.; Fujii, N. Pharmacophore identification of a specific CXCR4 inhibitor, T140, lead to development of effective anti-HIV agents with very high selectivity indexes. *Bioorg. Med. Chem. Lett.* **2000**, *10*, 2633–2637.
- (25) Tamamura, H.; Hiramatsu, K.; Ueda, S.; Wang, Z.; Kusano, S.; Terakubo, S.; Trent, J. O.; Peiper, S. C.; Yamamoto, N.; Nakashima, H.; Otaka, A.; Fujii, N. Stereoselective synthesis of [L-Arg-L/D-3-(2-naphthyl)alanine]-type (*E*)-alkene dipeptide isosteres and its application to the synthesis and biological evaluation of pseudopeptide analogues of the CXCR4 antagonist FC131. *J. Med. Chem.* **2005**, *48*, 380–391.
- (26) Tamamura, H.; Esaka, A.; Ogawa, T.; Araki, T.; Ueda, S.; Wang, Z.; Trent, J. O.; Tsutsumi, H.; Masuno, H.; Nakashima, H.; Yamamoto, N.; Peiper, S. C.; Otaka, A.; Fujii, N. Structure-activity relationship studies on CXCR4 antagonists having cyclic pentapeptide scaffolds. *Org. Biomol. Chem.* **2005**, *3*, 4392–4394.
- (27) Tamamura, H.; Araki, T.; Ueda, S.; Wang, Z.; Oishi, S.; Esaka, A.; Trent, J. O.; Nakashima, H.; Yamamoto, N.; Peiper, S. C.; Otaka, A.; Fujii, N. Identification of novel low molecular weight CXCR4 antagonists by structural tuning of cyclic tetrapeptide scaffolds. *J. Med. Chem.* **2005**, *48*, 3280–3289.
- (28) Marshall, G. R.; Wu, Y.; Heyden, N. V.; Ratner, L.; Nikiforovich, G. V. Backbone modification of cyclic pentapeptide antagonist of CXCR4. In *Peptides 2004 (Proceedings of 3rd international and 28th European peptide symposium)*; Flegel, M., Fridkin, M., Gilon, C., Slaninova, J., Eds.; Kenes International: Switzerland, 2005; pp 748–749.
- (29) Miller, S. C.; Scanlan, T. S. Site-selective N-methylation of peptides on solid support. *J. Am. Chem. Soc.* **1997**, *119*, 2301–2302.
- (30) Lin, X.; Dorr, H.; Nuss, J. M. Utilization of Fukuyama's sulfonamide protecting group for the synthesis of *N*-substituted  $\alpha$ -amino acids and derivatives. *Tetrahedron Lett.* **2000**, *41*, 3309–3313.
- (31) Carpino, L. A.; 1-Hydroxy-7-azabenzotriazole. An efficient peptide coupling additive. *J. Am. Chem. Soc.* **1993**, *115*, 4397–4398.
- (32) Bollhagen, R.; Schmiedberger, M.; Barlos, K.; Grell, E. A new reagent for the cleavage of fully protected peptides synthesised on 2-chlorotriethyl chloride resin. *J. Chem. Soc., Chem. Commun.* **1994**, 2559–2560.
- (33) Haubner, R.; Finsinger, D.; Kessler, H. Stereoisomeric peptide libraries and peptidomimetics for designing selective inhibitors of the  $\alpha_v\beta_3$  integrin for a new cancer therapy. *Angew. Chem. Int. Ed. Engl.* **1997**, *36*, 1374–1389.
- (34) Toniolo, C. Conformationally restricted peptides through short range cyclization. *Int. J. Pept. Protein Res.* **1990**, *35*, 287–300.
- (35) Dechantsreiter, M. A.; Planker, Eckart.; Matha, B.; Lohof, E.; Hölzemann, G.; Jonczyk, A.; Goodman, S. L.; Kessler, H. *N*-Methylated cyclic RGD peptides as highly active and selective  $\alpha_v\beta_3$  integrin antagonists. *J. Med. Chem.* **1998**, *42*, 3033–3040.
- (36) Rajeswaran, W. G.; Hocart, S. J.; Murphy, W. A.; Taylor, J. E.; Coy, D. H. Highly potent and subtype selective ligand derived by *N*-methyl scan of a somatostatin antagonist. *J. Med. Chem.* **2001**, *44*, 1305–1311.
- (37) Erchegeyi, J.; Hoeger, C. A.; Low, W.; Hoyer, D.; Waser, B.; Eltschinger, V.; Schaer, J.; Cascato, R.; Reubi, J. C.; Rivier, J. E. Somatostatin receptor 1 selective analogues: 2. *N<sup>α</sup>*-Methylated Scan. *J. Med. Chem.* **2005**, *48*, 507–514.
- (38) **32** exhibited two sets of signals in <sup>1</sup>H NMR spectra. The signals were assigned to *trans*- (69%) and *cis*- (31%) conformers at D-Tyr<sup>1</sup>-D-MeArg<sup>2</sup> amide bond. Since backbone conformation and side chain disposition of *cis*-conformer of **32** was apparently different from the parent peptides **2** and **3**, we assumed that the major *trans*-conformer could contribute to the bioactivities of **32**, although contribution of the minor *cis*-conformer cannot be ruled out.
- (39) Navenot, J. M.; Wang, Z. X.; Trent, J. O.; Murray, J. L.; Hu, Q. X.; DeLeeuw, L.; Moore, P. S.; Chang, Y.; Peiper, S. C. Molecular anatomy of CCR5 engagement by physiologic and viral chemokines and HIV-1 envelope glycoproteins; Differences in primary structural requirements for RANTES, MIP-1 $\alpha$ , and vMIP-II binding. *J. Mol. Biol.* **2001**, *59*, 380–393.

JM0607350